Advanced Steel Construction – Vol. 18 No. 1 (2022) 479–487
DOI:10.18057/IJASC.2022.18.1.6

A SIMPLE METHOD FOR A RELIABLE MODELLING OF THE NONLINEAR BEHAVIOUR OF BOLTED CONNECTIONS IN STEEL LATTICE TOWERS

Farshad Pourshargh [1], Frederic P. Legeron [1, 2], Sébastien Langlois [1, *] and Kahina Sad Saoud [1]

[1] *Université de Sherbrooke, Department of Civil and Building Engineering,*
2500 boul. de l'Université, Sherbrooke, QC J1K 2A1, Canada
[2] *PMC – Bridge & Tunnel UAE District Manager, Parsons, Abu Dhabi PO5498, UAE*
** (Corresponding author: E-mail: Sebastien.Langlois@USherbrooke.ca)*

ABSTRACT

The behaviour of bolted connections in steel lattice transmission line towers affects their load-bearing capacity and failure mode. Bolted connections are commonly modelled as pinned or fixed joints, but their behaviour lies between these two extremes and evolves in a nonlinear manner. Accordingly, an accurate finite element modelling of the structural response of complete steel lattice towers requires the consideration of various nonlinear phenomena involved in bolted connexions, such as bolt slippage. In this study, a practical method is proposed for the modelling of the nonlinear response of steel lattice tower connections involving one or multiple bolts. First, the local load-deformation behaviour of single-bolt lap connections is evaluated analytically depending on various geometric and material parameters and construction details. Then, the predicted nonlinear behaviour for a given configuration serves as an input to a 2D/3D numerical model of the entire assembly of plates in which the bolted joints are represented as discrete elements. For comparison purposes, an extensive experimental study comprising forty-four tests were conducted on steel plates assembled with one or two bolts. This approach is also extended to simulate the behaviour of assemblies including four bolts and the obtained results are checked against experimental datasets from the literature. The obtained results show that the proposed method can predict accurately the response of a variety of multi-bolt connections. A potential application of the strategy developed in this paper could be in the numerical modelling of full-scale steel lattice towers, particularly for a reliable estimation of the displacements.

ARTICLE HISTORY

Received: 11 December 2020
Revised: 26 May 2021
Accepted: 27 May 2021

KEYWORDS

Steel lattice tower;
Nonlinear behaviour;
Bolted connection;
Failure modes;
Bolt slippage;
Finite element modelling

1. Introduction

Steel lattice towers are widely used all over the world as transmission line supports. The structural integrity of such towers is a key factor in the reliability of a power transmission system. To minimize the risk of power supply disruptions that may occur because of tower failure, structural reliability of towers should be evaluated properly. In the standard simplified method of analysis and design, commonly used by tower engineers, lattice towers are idealized as linear trusses in which angle members are assumed to be connected to each other by frictionless joints acting as hinges. Moreover, the influence of end bending moments in members is generally ignored in simplified structural analyses, and leg members, which are supposed to be continuous, are assumed to be hinged in nodal points. Because of the simplifying assumptions used for design and analysis of lattice towers, it is a common practice among electric network operators to perform experimental tests on full-scale towers for the validation of new design concepts, which turns out to be a long and costly process.

Leg members in towers are connected via lap spliced bolted joints and the bracing members are usually connected to legs via single bolted joints to ensure a hinged connection. Assuming hinged joints does not represent their real behaviour and modelling bolted connections as rigid is also inadequate. In fact, an accurate numerical modelling of the behaviour of real joints is complex due to numerous interactions taking place locally.

The complex behaviour of bolted joints can be split into three categories: eccentricity, rotational stiffness and joint slippage. In practice, angle members in lattice towers are often loaded eccentrically, which causes a biaxial bending in addition to axial loads. The combined action of axial and bending forces may cause a plastic hinge in the cross-section and the bolted leg of the angle could undergo a local post-elastic deformation under the bearing force of bolts, causing displacement and rotation in the connection and shear lag in the member [1].

Additionally, most of the bolt holes are in practice slightly larger than the diameter of bolts, which makes joint slippage inevitable. The slippage may happen gradually or at a specific level of loading and it depends on different parameters such as: structural loading, workmanship, the constitutive properties of the bolts and connections, nature and condition of the faying surfaces and bolt torqueing [2, 3].

Because of the lack of experimental data and the complexity of describing the actual slippage phenomenon in a real structure, simplified models have to be used. For example, in a study by Kitipornchai et al. [4], the slippage is modeled as a random process. The authors concluded that joint behaviour does not have a significant influence on the ultimate strength of the structure, but it influences deflections. In a comparison of numerical predictions with experimental results, Jiang et al. [5] investigated the effect of joints on structural analysis model. The results of their study showed that to predict the tower sway displacement, joint behaviour must be considered. This will drastically increase the predicted tower deformation but will not affect its failure load, failure mode and sequence. In a subsequent study, Jiang et al. [6] numerically investigated the impact of the combination of various joint effects, including connections' semi-rigidity, joint slippage, and initial geometric imperfections, on the structural behaviour of an ultrahigh-voltage steel lattice tower. Their study revealed second order effects should be considered to accurately predict the behaviour of slender transmission line towers.

To account for the joint stiffness, Kang et al. [7] found that the connection rigidity may have a considerable effect on the ultimate horizontal loading capacity of a lattice tower. The rigid connection increases the buckling capacity, thus the assumption on connection rigidity must be realistic. Otherwise, the buckling capacity of the structure may be over or underestimated.

Knight and Santhakumar [8] concluded that neglecting the joint effects may be responsible for the premature failure in towers and must thus be considered in the analysis. The results of their study showed a good correlation with experiments when joint effects are considered. An et al. [9] carried out an experimental and numerical study on the nonlinear axial stiffness of multi-bolted leg joints typically employed in classical 500 kV lattice transmission towers in China. A simplified model was also proposed in this study for the characterization of the load-deformation relationship. However, the proposed model does not cover configurations including a reduced number of bolts, which is commonly the case in steel lattice transmission line towers. Ungkurapinan et al. [10] investigated the behaviour of various configurations of connections involving one to four bolts. Unfortunately, there is not a complete database of slippage parameters for angle member connections. Some limited numbers of tests are available on specific angle sections and bolt arrangements. From the literature, it is observed that the behaviour of bolted joints influences deflections of steel lattice towers most of the time, and failure modes and ultimate loading only in some cases. It is recognized that the tower connections are different from ordinary steel connections in other types of steel structures [10].

In lattice transmission towers, the members are mostly connected directly via their flange or through the gusset plates which provide a connection flexibility. In addition, the slippage effect should be included in the numerical model, because lattice towers are constructed by bearing type connections instead of friction type ones. In this respect, recent studies conducted by Abdelrahman et al. [11], and Gan et al. [12], among others, have highlighted the

importance of appropriately considering the influential factors in the design process.

The general objective of this article is to propose a simple method to predict the complex behaviour of bolted connections in steel lattice towers. The procedure detailed in this paper comprises two main aspects. First, the nonlinear load-deformation behaviour of single-bolt connections is characterized based on their geometric/material properties and some construction details. This characterization includes the identification of the pre-slip, slip and post-slip regions of the behaviour. Then, the calculated behaviour is applied to finite element models of bolted assemblies, where the connections are represented using nonlinear spring elements. The finite element method can involve multiple bolts with various arrangements. The accuracy of developed method is verified by conducting experimental tests on plate assemblies including single-bolt and two-bolt configurations. The prediction method is also compared to datasets from experimental tests performed on four-bolt connections provided by Cai and Driver [13] as well as a detailed three-dimensional finite element modelling of two-bolt connections considering multiple interactions between the assembled plates and the bolts.

The proposed method is intended to be easily implemented for a wide range of joint configurations and may find broader application in the context of numerical modelling of complete lattice towers with the aim of evaluating precisely their complex structural behaviour.

This article starts by presenting the approach developed for the representation of the behaviour of multi-bolt connections. Then, the experimental program investigating the response of different plate assemblies involving one or two bolts is briefly described. Finally, various configurations involving single and multiple bolts are examined and the obtained numerical results are compared with reference results.

2. Modelling and prediction of the nonlinear behaviour of bolted connections

In the present study, a nonlinear discrete element is employed to model the bolted connections. The paper particularly investigates the effect of varying the following geometric parameters: the plate thickness t_p, the plate width W, the bolt diameter D, the end distance of plate (distance from the center of the hole to plate edge) L_e, and the number of bolts n (the configurations analysed are summarized in Table 1 and Table 2). The nonlinear spring element should also be able to include the deflection due to slippage of connection and the near-field behaviour of plate in the vicinity of the bolt. The local behaviour of single-bolt connections, from loading to failure, is first predicted analytically as described subsequently. Then, the predicted load-deformation law is applied to numerically model the nonlinear response of plate assemblies using nonlinear spring elements. Code_Aster [14], an open-source finite element software package developed by "Electricité de France" (EDF), is used in this research. Code_Aster [14] has a powerful nonlinear spring element that can model the connection behaviour. The methodology is to first predict the behaviour of single-bolt connection using equations available in the literature based on its properties and considering the near-field behaviour. At the second step, a series of specimens is tested in laboratory to validate the prediction model. The third step proposes a method to categorize multi-bolt connections and predict their behaviour based on one bolt predicted model. This step is done with the help of a finite element plate model. At the next step, the method is evaluated by conducting experiments on several two-bolt joints. In the final step, predictions are compared to experimental results of four-bolt connection tests which have been reported by a research at the University of Alberta, Canada [13].

2.1. Prediction method for one-bolt connections

Fig.1 illustrates the typical force-displacement relationship of a bolted connection under uniaxial tensile load. This graph may be divided into two main regions: pre-contact and post-contact. The pre-contact region is characterized by a frictional load transfer followed by a significant bolt slippage and ends at the contact point defining the threshold value for establishing contact between the bolt and the plate. Beyond the contact point begins the post-contact region, in which the load is mainly transferred by bearing up to the failure of the joint.

To characterize the local response of a bolted connection, the values of the load at which bolt slippage occurs P_{slip}, the peak load $P_{failure}$, the elastic displacement reached before the onset of slippage $D_{preslip}$, the displacement at the end of the pre-contact region D_{slip} and the ultimate displacement $D_{failure}$ should first be determined based on the geometric and material properties of the connection and some construction details.

Once evaluated, the parameters defining the curve depicted in Fig.1 will be used in a two-dimensional finite element model, where the bolted joints are represented using spring elements, to deeply investigate the global response of assemblies. This may be done by assigning these values to the discrete elements through the nonlinear behaviour law ASSE_CORN implemented in Code_Aster [14].

To determine the limit values associated with the pre-contact region, it is proposed to use equations developed by Rex and Easterling [15] to predict the slip behaviour of a single bolt bearing on a plate. They proposed the value of 0.193 mm for $D_{preslip}$ based on various experiments performed on a single plate assembled using one bolt. D_{slip} directly depends on the bolt hole clearance. Normally, the bolt holes are drilled larger than the diameter of bolts to satisfy the requirements in terms of erection tolerance. For example, common industry practices consider the value of 1.6 mm as a standard hole clearance in North American steel construction. Unless otherwise specified, the values of $D_{preslip}$ and D_{slip} in this work will be taken as 0.193 mm and 1.6 mm respectively.

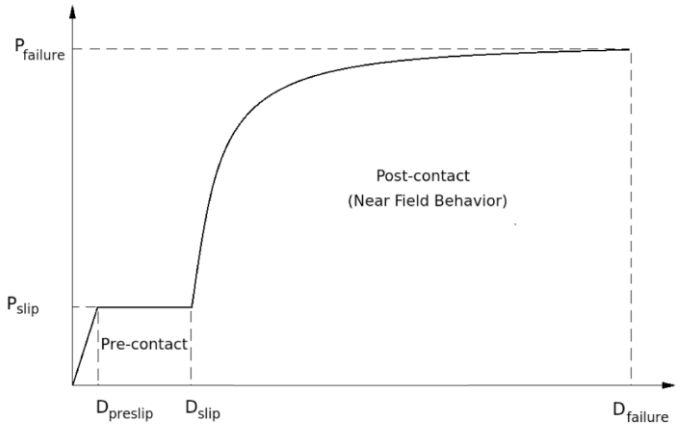

Fig. 1 Behaviour of connection under axial load

The value P_{slip} is here calculated using the method of AISC code [16] as follows:

$$P_{slip} = K_s \times m \times n \times T_i \tag{1}$$

Where:

$$T_i = \frac{Bolt\ Torque}{C \times D} \tag{2}$$

And m = number of slip surfaces (two for the cases handled in this paper), n = number of bolts (one bolt in this case); K_s = slip coefficient (for a typical steel surface, K_s is taken as 0.33); C = nut factor (0.2, as given by [17]); and D = bolt diameter.

The amount of bolt torque in equation (2) is taken as 100 N-m, in accordance with the experimental tests carried out in this study.

For the post-contact region, the following empirical equation proposed by Rex and Easterling [18] will be used to predict the behaviour of a single-bolt connection [following equations use units of mm and kN]:

$$\frac{R}{R_n} = \frac{1.74 \times \bar{\Delta}}{(1+(\bar{\Delta})^{0.5})^2} - 0.009 \times \bar{\Delta} \tag{3}$$

In which, R is the plate load, and R_n the plate nominal strength which may be evaluated as follows:

$$R_n = D \times t_p \times F_b \tag{4}$$

And $\bar{\Delta}$ is the nominal deformation which is defined in equation (5).
In equation (4), the bearing/tear-out strength of the plate F_b is defined by the following relationship:

$$\bar{\Delta} = \frac{\Delta \times \beta \times K_i}{R_n} \tag{5}$$

$$F_b = F_u \times \frac{L_e}{D} \leq 2.4 \times F_u \tag{6}$$

$$K_i = \frac{1}{\frac{1}{K_{br}} + \frac{1}{K_b} + \frac{1}{K_v}} \tag{7}$$

$$K_{br} = 120 \times t_p \times F_y \times (D/25.4) \tag{8}$$

$$K_b = 32 \times E \times t_p \times (L_e/D - 1/2)^3 \tag{9}$$

$$K_v = 6.67 \times G \times t_p \times (L_e/D - 1/2) \tag{10}$$

In equation (5), Δ stands for the hole elongation and β denotes the steel correction factor, which is taken as 1.0 for typical structural steel. Equation (7) evaluates the initial stiffness of the connection K_i, from the bearing stiffness K_{br}, the bending stiffness K_b, and the shearing stiffness K_v. In this analysis, the modulus of elasticity E and the shear modulus G of steel are taken equal to 210,000 MPa and 80,000 Mpa, respectively. The material grade of steel plates is CSA-G40-400W and the bolt grade is ASTM-A325

2.2. Prediction method for multi-bolt connections

The main contribution of this research is to predict the behaviour of multi-bolt connections based on the near field behaviour of one bolt. None of the literature reviewed considered the prediction of full behaviour for the connections. In this section, the behavior of multi-bolt connections is predicted. The behaviour of one-bolt joint is applied to a finite element model through a nonlinear spring element. The properties of the spring elements are determined according to the method discussed in the previous section.

The finite element model is built using quadrilateral shell elements named "DKT" in Code_Aster [14]. Each element has four nodes with six degrees of freedom and a bi-linear behaviour law is considered for the inelastic material. The mesh size is adjusted considering geometrical complexity of the model, especially around holes. Mesh refinement is applied where needed based on a preliminary mesh size sensitivity analysis and the mesh size varies between 4 mm and 10 mm. Fig.2 compares the results obtained for a connection involving two bolts based on three mesh trials. In this case, since the nonlinearity is mostly due to the spring elements, mesh size and density does not have a noticeable effect on the behaviour. The central nodes of bolts are represented as fixed support and a uniformly distributed tensile load is applied on the right side of the model. In reality, the near field zone is connected continuously to the surrounding area on the plate. To capture this, a rectangular cut out is created which provides extra nodes from the finite element model to connect the spring and avoid stress concentration. The rectangular shape also makes the mesh more structured. To illustrate this point, an example of a two-bolt connection is shown in Fig.3. The green lines in the figure, represent the rigid link elements to connect the non-linear spring element to nodes of near field behaviour zone. The rigid links work under tension and compression and they link the degrees of freedom of two nodes.

The model is also able to consider different types of bolts with different diameters in the same connection. The near field behaviour of one bolt can be predicted first based on the method described in section 2.1 and then it will be assigned to nonlinear spring elements, in any location on the plate. The efficiency of the proposed method is evaluated in section 4.3 by comparing to the tests on 4 two-bolt connection configurations.

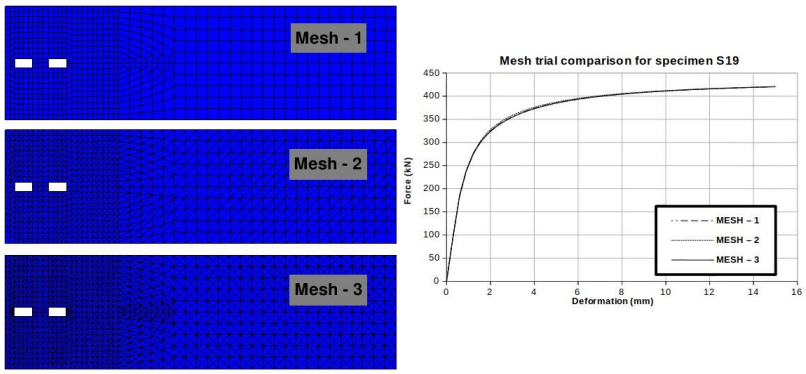

Fig. 2 Comparison of different mesh refinement and sizes

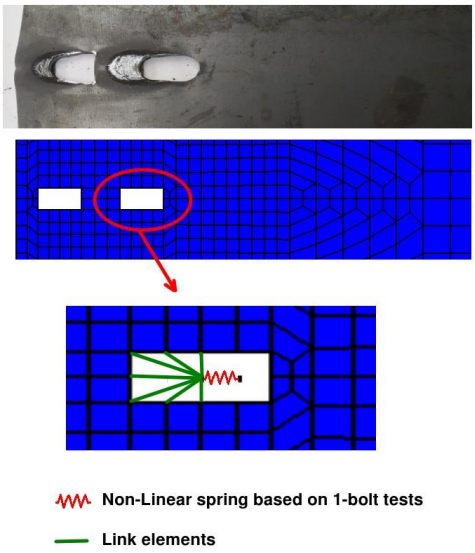

Fig. 3 2D modelling of a two-bolt connection using a plate and spring elements

The method proposed in this study is also verified by predicting the response of 10 four-bolt specimens which have been tested by Cai and Driver [13]. The researchers have used I-sections with bolt holes in the web, and the sections were loaded in tension to determine the capacity of connection. Fig.4 shows one of the specimens and the geometry of model which is proposed for the prediction. As one can notice, the four-bolt configuration presented in Fig.4 is not representative of lattice towers' typical connections. The main purpose here is to take advantage of the experimental results reported in the article by Cai and Driver [13] in order to evaluate the reliability of the method proposed in this paper. Three-dimensional shell elements of Code_Aster [14] were used to mesh the model due to the complex geometry of the analysed samples. Each element has nine nodes with six degrees of freedom per node. The central node of bolts is modeled as a fixed support and a uniformly distributed tensile load is applied to the nodes located at the free end of the I-sections. The size of the near field zone in this case is equal to edge distance of the bolt hole. In this case, the spring is connected to the sides of the zone since the end distance was too small to provide adequate support at the end of the rectangular holes (see Fig. 4).

The prediction method and procedure for these specimens is the same as two-bolt specimens. First, the near field behaviour of one bolt is calculated using equations 1 to 3. Then the behaviour is applied to the four-bolt model through the nonlinear spring elements. Properties of the specimens analysed are presented in Table 1 and Fig. 5.

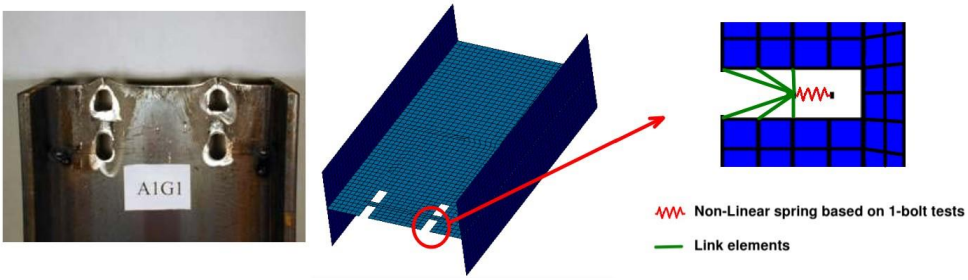

Fig. 4 FE modelling of a connection involving four bolts

Table 1
Properties of four-bolt specimens [8]

Section	D (mm)	W (mm)	t_p (mm)	L_e (mm)	*Fy* (MPa)	*Fu* (Mpa)
A1G1	19	305.4	7.48	28.3	439	519
A2G1	19	305.4	7.52	29.27	439	519
A7G1	19	304	7.43	28.55	411	494
A5E1	19	248.5	7.55	31	343	487
A11E1	19	249.9	7.30	28.27	376	500
A8G2	19	304.5	7.44	27.08	411	494
A3R1	19	310	6.30	28.15	379	472
A9R1	19	311.6	6.54	27.56	369	478
A6E2	19	248	7.51	47.73	343	487
A12E2	19	249.5	7.34	44.0	376	500

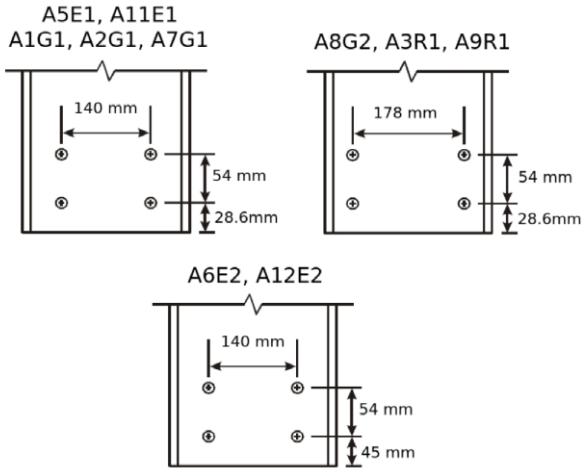

Fig. 5 Configuration of four-bolt specimens [8]

3. Experimental program

This section reports the experimental investigations carried out on double lap connections. These tests will serve for the validation of the method developed in this paper for the prediction of the complex behaviour of multi-bolt connections.

3.1. Specimens

In this research, bolt plate specimens were tested under uniaxial tensile loading. The experimental program consists of eighteen one-bolt and four two-bolt configurations. To ensure the quality and the reproducibility of the results, each configuration was tested twice. Fig.6 summarizes the dimensions and configurations of test specimens.

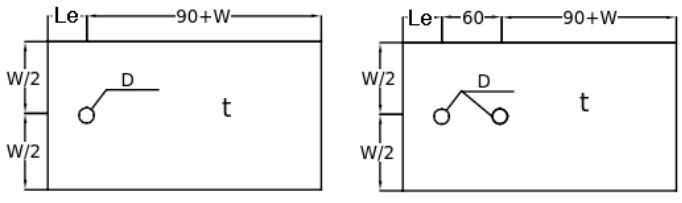

Fig. 6 Configuration of the tested specimens

The one-bolt specimens were used to validate the analytical modelling method proposed in this article. A uniaxial load was applied to all of the specimens. The main variables are plate thickness, plate width, bolt diameter and end distance. The specimens were designed to fail under three different failure modes: (i) bearing; (ii) cleavage and (iii) end bearing [16]. The complete description of one-bolt specimens is provided in Table 2. The second group of specimens were designed to evaluate the prediction method for two bolts. These specimens were designed in a way that the near field behaviour of bolts is already predicted from the previous one-bolt tests. The objective is to define a prediction method for connections with more bolts based on near field behaviour of one bolt. The properties for this group of tests are provided in Table 3.

Table 2
Properties of one-bolt test specimens

Configuration	D (mm)	W (mm)	t_p (mm)	L_e (mm)	F_y (MPa)	F_u (Mpa)	Failure Scenario
S1	16	152	9.5	40	396	555	B
S2	16	127	9.5	40	404	529	B
S3	16	127	7.9	40	417	560	B
S4	19	152	9.5	47.5	396	555	B
S5	19	127	9.5	47.5	404	529	B
S6	19	127	7.9	47.5	417	560	B
S7	16	152	9.5	24	396	555	C+S
S8	16	127	9.5	24	404	529	C+S
S9	16	89	6.35	24	370	578	C+S
S10	19	152	12.7	28.5	383	520	C+S
S11	19	127	7.9	28.5	417	560	C+S
S12	19	89	6.35	28.5	370	578	C+S

Note: (B: Bearing failure, C+S: Cleavage and End shear failure)

3.2. Test set-up

The specimens were tested in a tension jig. To prevent the prying action of plates, the setup was prepared so as to apply only a uniaxial force on the specimens, without eccentricity or bending moments. Fig.7 and Fig.8 show the layout of experimental setup.

Plates PL-2 and PL-3, were used in all the test cases, but PL-1 was changed according to the thickness of each specimens. The thickness of plates PL-2 and PL-3 is 25mm and they are connected to PL-1 by six M16 bolts. The dimensions of the plates are 500 mm for length and 250mm for width. Each bolt was tensioned manually to a torque of 100 N-m to match common practice in the transmission line industry. To acquire accurate torque, a calibrated torque wrench was used. All the surfaces are normal bare steel without any preparation.

To measure the deformation of specimens, a high accuracy laser displacement transducer was used. The transducer rested on PL-2 or PL3 and the probe mounted on the specimen by using a small aluminium angle. Therefore, the relative deformation between the specimen and the connection plates was measured accurately. Fig.3 shows the set-up and location of displacement transducer.

An MTS hydraulic testing machine was used to apply tension to specimens. The capacity of the machine is 500 kN. The loading was displacement controlled with a loading rate of 1mm/min. The maximum value of displacement that was provided by the machine was set equal to the bolt diameter, although most of the specimens failed before this value was reached.

Table 3
Two-bolt test specimens

Configuration	Corresponding one-bolt configuration	D (mm)	W (mm)	t_p (mm)	L_e (mm)	F_y (Mpa)	F_u (Mpa)	Failure Scenario
S19	S1	16	200	9.5	40	387	516	B
S20	S3	16	200	7.9	40	452	482	B
S21	S4	19	250	9.5	47.5	374	521	B
S22	S6	19	250	7.9	47.5	390	465	B

Note: (B: Bearing failure)

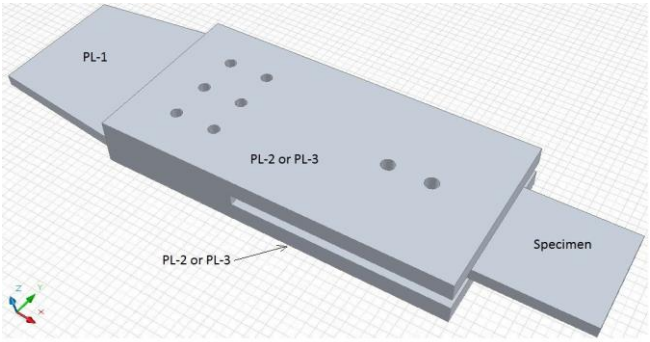

Fig. 7 Layout of experimental set-up

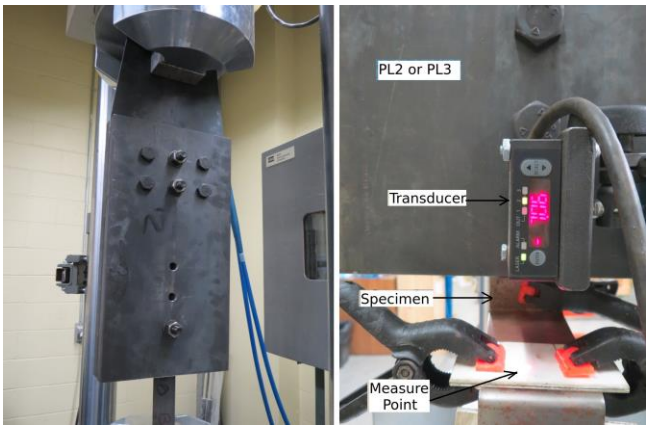

Fig. 8 Final setup and transducer location

3.3. Material property tests

Two tension coupons were cut and prepared from each batch of steel material and tested according to ASTM A370-02 standard [19]. The values of yield strength F_y and ultimate tensile strength F_u of steel obtained from tensile coupon tests were used in the prediction method. These values are indicated in Tables 1 and 2.

4. Results and discussion

4.1. Analysis of configurations involving one bolt

Figs. 9a and 9b depict the force-displacement curves of twelve one-bolt specimens (S1 to S12). These figures show that the proposed method can predict the full behaviour of the connections with high accuracy compared to the results obtained from the experimental tests. The predicted curve is also able to consider slip behaviour during the loading phase and the trend of the curve is similar to the behaviour of specimens. As shown in Fig. 3, the specimens in this study were tested using a vertical test setup and the effect of gravity minimized the gap between the bolt and the contact surface of the hole. So in this case, to have a more realistic evaluation of the force-deflection relationship, the value of 1.6 mm gap is not introduced to the prediction method. As a result, the slippage behaviour is not significant in the predictions. The pre-tensioning force in the bolts also causes the slippage to happen gradually.

In Figs. 9a and 9b, the predicted curves are stopped at a displacement equals to bolt diameter because the method does not provide an estimate for final displacement. Even though the objective of this research is to predict the complete behaviour of connection, it is clear that the method can provide the values of ultimate capacity with a significant accuracy. Table 4 presents a comparison for the ultimate capacity between the prediction method and the experimental tests. The ratio of prediction to test capacity is on average 0.98. The following symbols are used in the tables, P_{ut} (ultimate capacity of test specimens), D_{ft} (final deflection of test specimens), P_{upr} (ultimate capacity predicted by the method). It is clear from Fig. 9b, that while the maximum load is well captured for all failure modes tested (B or C+S), the ultimate displacement is not captured accurately by the method for mode C+S.

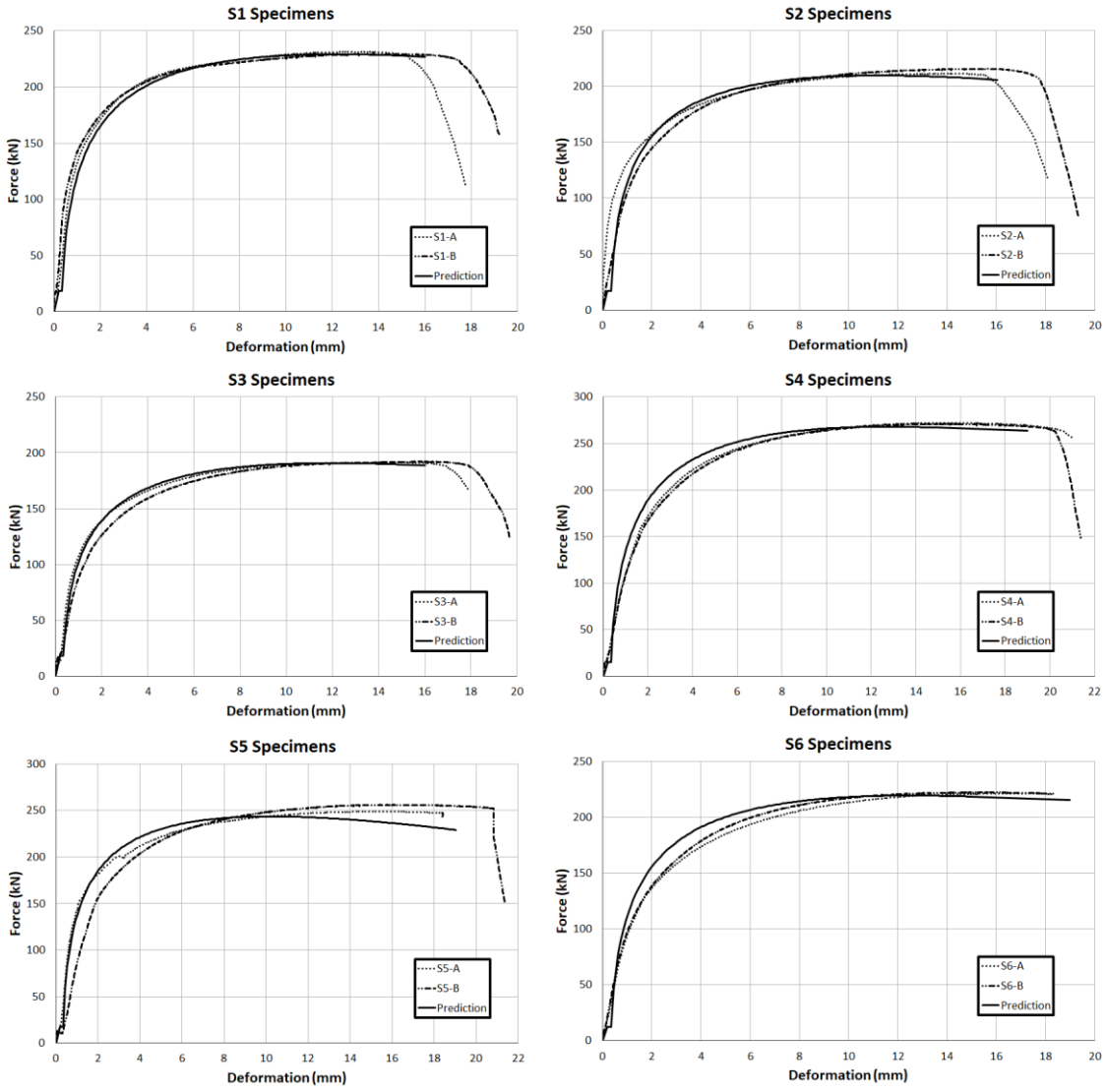

Fig. 9a Comparison of prediction and experimental behaviour of single-bolt connections

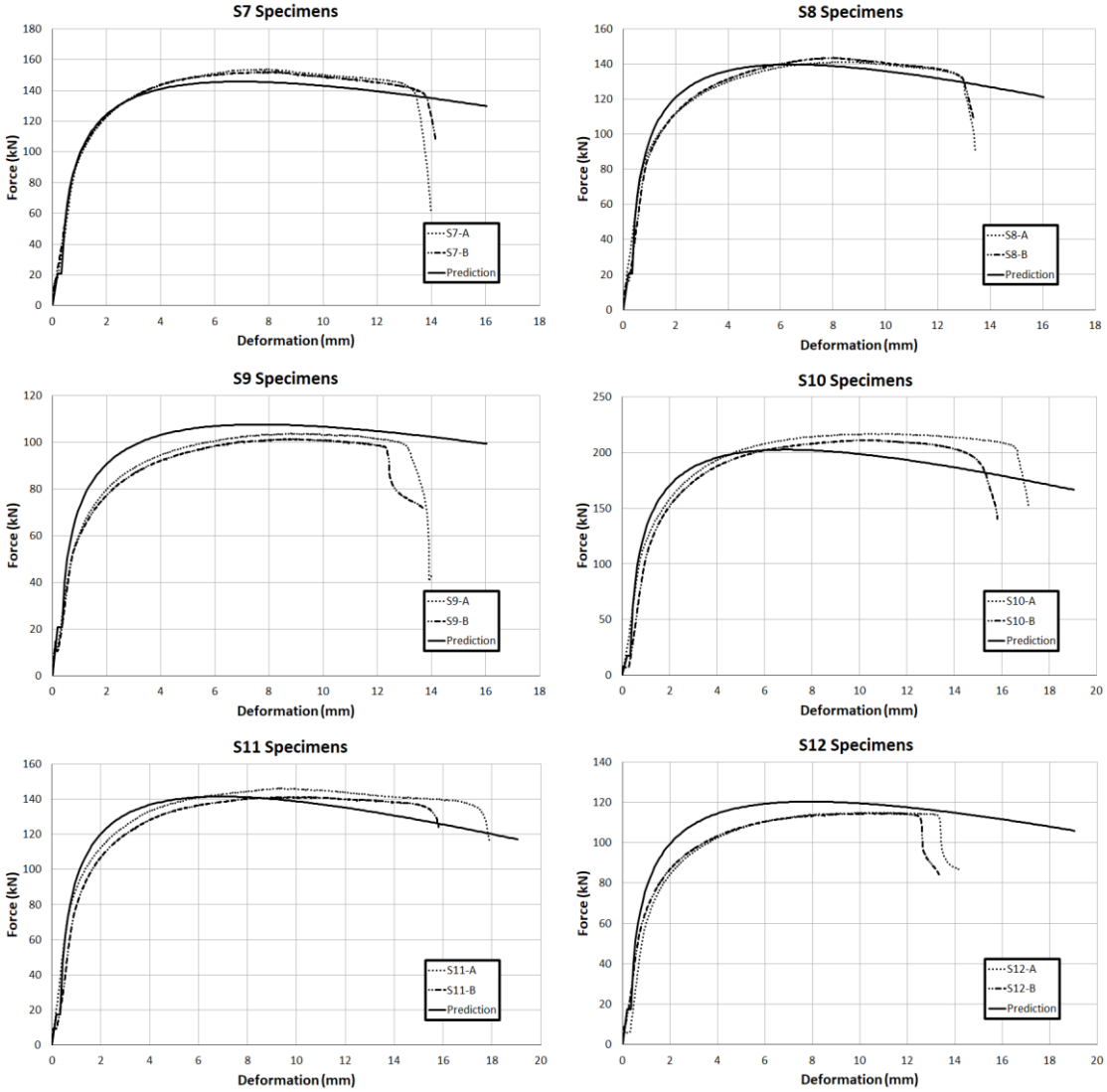

Fig. 9b Comparison of prediction and experimental behaviour of single-bolt connections

Table 4
Comparison of predicted and experimental ultimate capacity for one-bolt specimens

Specimen	P_{ut} (kN)	D_{ft} (mm)	P_{upr} (kN)	P_{upr}/P_{ut}
S1	230	16	219	0.95
S2	214	16	209	0.98
S3	192	17	188	0.98
S4	272	18	255	0.94
S5	253	18	244	0.97
S6	222	18	217	0.98
S7	153	13	146	0.95
S8	142	12	140	0.98
S9	103	12	107	1.04
S10	214	15	203	0.94
S11	144	15	142	0.99
S12	115	12	120	1.05
Average				0.98
COV (%)				3.6

COV: Coefficient of variation

4.2. Analysis of configurations involving two bolts

The method proposed for the prediction of the behaviour of connections with two bolts is derived using a finite element model. As described previously, the near field behaviour of each bolt was assigned to the model by means of a nonlinear spring and the remaining parts of the specimen were modelled by shell elements. The prediction of specimen S19 has been performed based on the predicted near field behaviour of S1, which has the same bolt diameter, plate thickness, plate width and end distance. Similarly, the specimens S20, S21 and S22 have been predicted based on S3, S4 and S6 predictions, respectively.

In addition a detailed 3D numerical modelling of the analysed two-bolt samples is performed in this case using three-dimensional solid finite elements. Fig.10 shows the geometry and mesh of the model. The numerical model is developed using Code_Aster [14] and the adopted mesh scheme is constituted of 8-node isoparametric brick elements. To diminish the computational costs, each component of the connections is meshed individually with a fine mesh around the contact area and a coarse mesh elsewhere. In this formulation, the principle of virtual work is expressed in the current configuration accounting for finite strains. The inelastic behaviour of the structural steel composing the plates is approximated by a multi-linear stress-strain relationship derived from the tensile coupon tests carried out on the analysed specimens (S19 to S22). In the absence of relevant details on the material behaviour of the high-strength bolts, they are modelled using a bi-linear elastoplastic constitutive law characterised by the modulus of elasticity E=200 GPa, Poisson's ratio ν=0.3, yield strength F_y=800 MPa, and the tangent modulus H=1 MPa. Finally, the von Mises yield criterion in conjunction with a linear isotropic hardening rule is adopted herein to simulate the plastic behaviour of the steel.

Plate PL-1 shown in Fig.7 is not represented in this modelling as it does not produce any direct effect on the behaviour of the connection. In accordance with the experimental tests, the uniaxial tensile loading is applied as an imposed displacement, while the surfaces of plates PL-2 and PL-3 are fully clamped in the side opposite to the loaded surface. The different parts constituting each connection are assembled using two bolts and the contact/friction behaviour, between plates PL-2/PL-3 and the bolts' head/washer, the three plates and the bolts' shank, and at interfaces between the central plate and plates PL-2/PL-3, is treated using the augmented Lagrangian method.

Fig.11 illustrates the comparison of the axial load-displacement results for the tests conducted on specimens with two bolts (S19 to S22). The numerical and experimental deformed configurations of the specimen S20, for instance, are shown in Fig.12. From Fig.12 it may be observed that the proposed method (Fig.12b) is in line with the experimental (Fig.12c) and the numerical (Fig.12a) deformed shapes.

As shown in Fig.11, good agreement is generally obtained between the developed method (using shell elements) and the experimental tests.

For specimen S21, the final displacement measured experimentally is smaller than the expected value. Since the operational capacity of testing machine was about 450 kN, this test was terminated to avoid damage to the machine. Also, one of the experimental tests performed on specimen S21 provided unreliable output due to misalignment of transducer. Therefore, only one experimental load-displacement curve is presented for this configuration. By contrast, the numerical results obtained using 3D solid elements are somewhat different from the experimental ones.

Despite its simplicity, the proposed method thus appears to be computationally more efficient than a detailed numerical modelling using three-dimensional solid elements. Finally, Table 5 summarizes the ultimate capacity obtained with the proposed method. Average difference of connection capacity between the prediction method and experimental results is 2 percent.

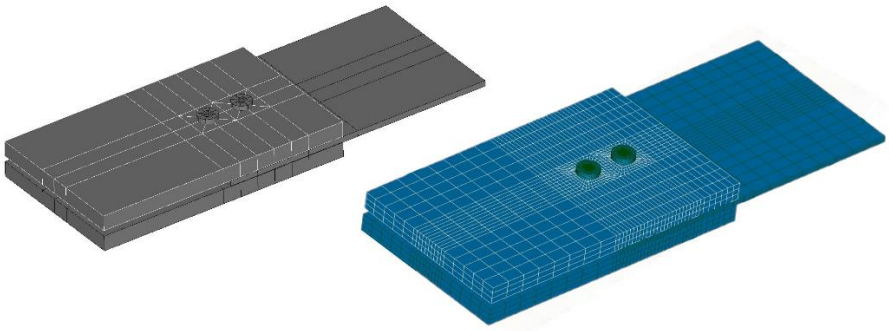

Fig. 10 Numerical model of the two-bolt tests using 3D solid elements

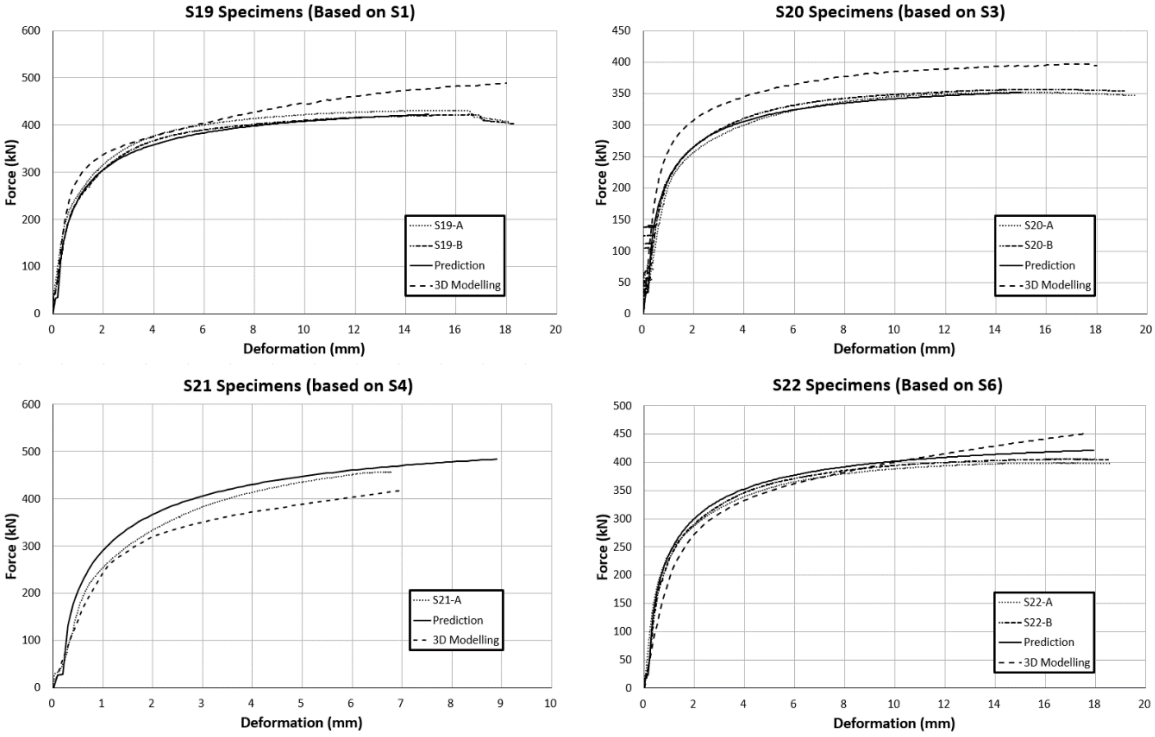

Fig. 11 Comparison of two-bolt connections

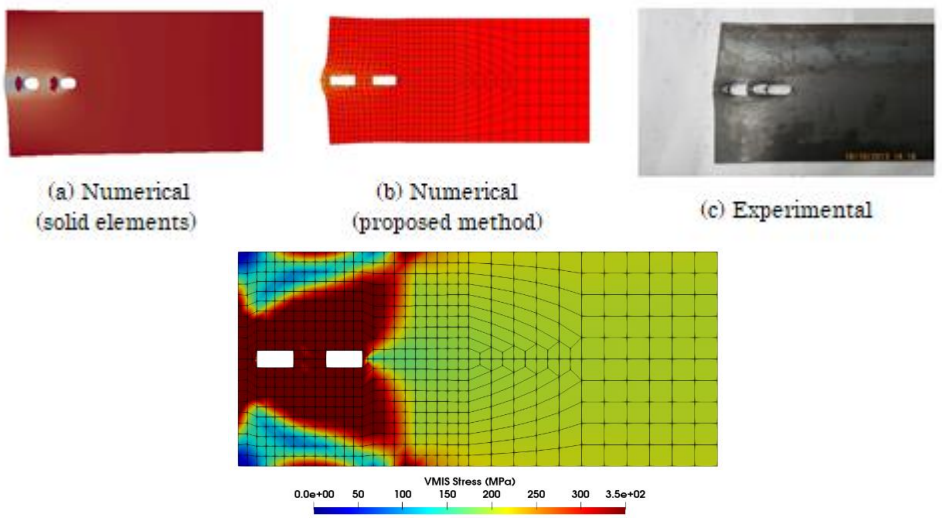

Fig. 12 Deformed configuration and yielding stress map of a two-bolt connection (specimen S20)

Table 5
Comparison of predicted and experimental ultimate capacity for two-bolt specimens

Specimen	P_{ut} (kN)	D_{ft} (mm)	P_{upr} (kN)	P_{u_3D} (kN)	$\frac{P_{upr}}{P_{ut}}$
S19	427	17	420	486	0.98
S20	354	19	363	397	1.03
S21	450	6.79*	475	417	1.06
S22	402	19	420	451	1.04
Average					1.02
COV (%)					3.31

P_{ut}: ultimate capacity of test specimens
D_{ft}: final deflection of test specimens
P_{upr}: ultimate capacity predicted by the method
P_{u_3D}: ultimate capacity of FE model using 3D solid elements
COV: Coefficient of Variation
* This specimen did not reach complete failure due to capacity of testing machine

4.3. Analysis of configurations involving four bolts

Fig.13 compares the predictions of four-bolt specimens with the tests results of the study from Cai and Driver [13]. Table 6 summarizes the results for the ten specimens considered in this study. Since the size of bolt hole for each specimen was not mentioned in their report, the amount of D_{slip} parameter is considered approximately to fit the experimental results. This set of tests also shows that the method can predict the behaviour of multi-bolt connections with acceptable accuracy. As it is observed from Table 6, the prediction method underestimates the ultimate capacity by 12 percent on average. The slippage behaviour of specimen A8G2 is obvious for both test and predicted results.

Table 6
Comparison of predicted and experimental ultimate capacity for four-bolt specimens

Specimen	P_{ut} (kN)	D_{ft} (mm)	P_{upr} (kN)	$\frac{P_{upr}}{P_{ut}}$
A1G1	691	14	610	0.88
A2G1	724	9	675	0.93
A7G1	665	16	645	0.97
A5E1	698	9	600	0.86
A11E1	691	14	600	0.87
A8G2	622	12	611	0.98
A3R1	634	11	475	0.75
A9R1	633	16	500	0.79
A6E2	776	7	680	0.88
A12E2	793	16	715	0.90
Average				0.88
COV (%)				8.15

COV: Coefficient of variation

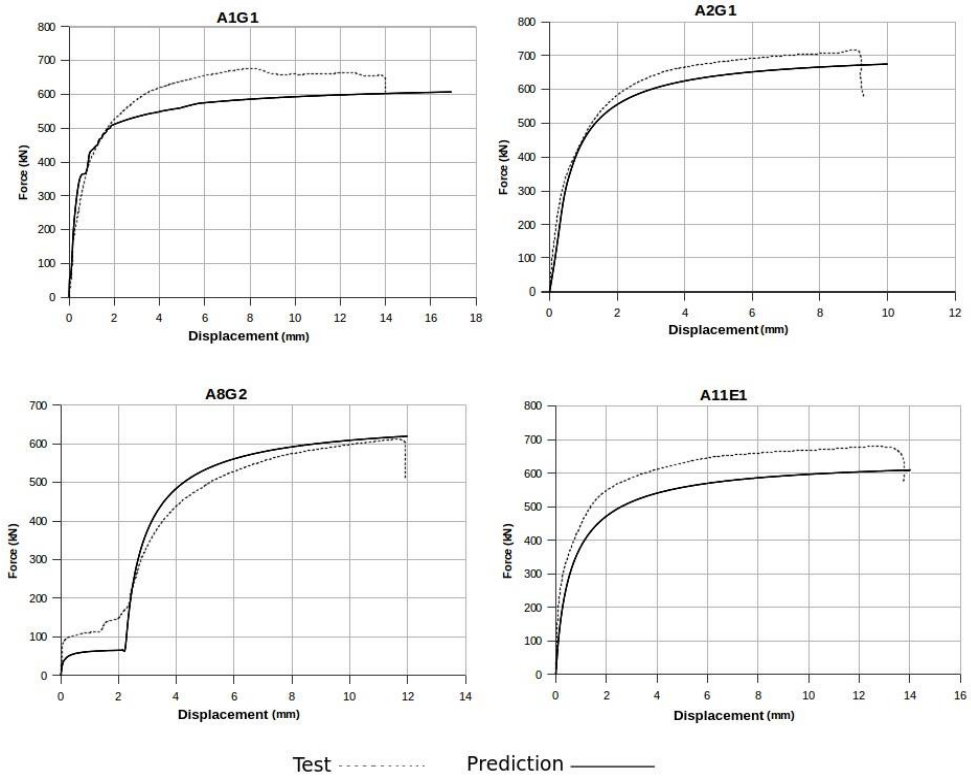

Fig. 13 Comparison of four-bolt Specimens

4.4. Potential application of the proposed method in modelling of a steel lattice tower

Once the nonlinear behaviour of multi-bolt connections is predicted using the method described in sections 4.2 and 4.3, one may take advantage of these results to accurately analyse the structural behaviour of lattice structures. Depending on the software used, this can be done by introducing the full curve of the connection's behaviour or, as it is done in Code_Aster [14], by introducing the key parameters defining the curves, as described in sections 4.2 and 4.3. The proposed method allows to obtain the properties for a unique spring element that captures the overall nonlinear behaviour of a given multi-bolted connection. This spring can easily be implemented at the end of a beam element in a complete lattice tower model.

The parameters to be evaluated are P_{slip}, $P_{failure}$, D_{slip} and $D_{failure}$, and should be assigned to each spring element. Let us recall that the parameters $P_{failure}$ and $D_{failure}$ are the maximum capacity of the connection and the corresponding displacement, respectively. The values of P_{slip} and D_{slip} depend on the amount of slippage in the connections. If there is substantial and obvious slippage in the predicted behaviour, these values can be extracted directly from the curve. Otherwise, these values are assumed to be zero which means that near field behaviour initiates from the beginning and there is no slippage. Tables 7 and 8 indicate the mentioned parameters to calibrate nonlinear springs for two-bolt and four-bolt connections of this study.

Table 7
Parameters to calibrate the nonlinear spring (two-bolt)

Specimen	P_{slip} (kN)	D_{slip} (mm)	$P_{failure}$ (kN)	$D_{failure}$ (mm)
S19	0	0	420	15
S20	0	0	363	15
S21	0	0	475	9
S22	0	0	420	19

Table 8
Parameters to calibrate the nonlinear spring (four-bolt)

Specimen	P_{slip} (kN)	D_{slip} (mm)	$P_{failure}$ (kN)	$D_{failure}$ (mm)
A1G1	0	0	610	17
A2G1	0	0	675	10
A7G1	65	2.1	645	16
A5E1	0	0	600	9
A11E1	0	0	600	14
A8G2	66	2.2	611	12
A3R1	0	0	475	12
A9R1	0	0	500	15
A6E2	0	0	680	8
A12E2	0	0	715	15

5. Concluding remarks

This article presents a method to predict the full force-deformation behaviour of multi-bolt connections under uniaxial tension. The method is based on adding the near field behaviour of each bolt through a nonlinear spring element in the finite element model of the connection. Several experimental tests on single-bolt connections were conducted and the results showed that their behaviour can be evaluated with existing theoretical and empirical relations. The near field behaviour is then applied as a nonlinear spring to the finite element model of various connections. Next, the results for the finite element model were compared to experimental tests performed on two-bolt connections and to existing four-bolt tests. The method accurately predicted the full behaviour of one-, two- and four-bolt connections with different configurations and properties. It also allowed to match closely the ultimate capacity of the connection.

The proposed method allows to predict the full force-displacement curve of multi-bolt connections using a finite element model and starting from the geometry and mechanical properties of each individual bolt. This force-displacement curve for the multi-bolt connection can be used to calibrate a nonlinear spring that will reproduce the connection behaviour in a large-scale tower model. For future work, more experimental tests with different bolt numbers and arrangements should be conducted. Also, tests on models should be performed to study the rotational behaviour of steel angle connections. Moreover, this study focused on bearing and end-shear failure. For the net section failure, another approach needs to be developed. It is also recommended that the predictions of the present study be applied to a finite element model of a complex lattice tower and compared to full scale experimental tests.

References

[1] N. Prasada Rao, S. J. Mohan, N. Lakshmanan, A study on failure of cross arms in transmission line towers during prototype testing, International Journal of Structural Stability and Dynamics 5 (3) (2005) 435–455.
[2] W. Kang, F. Albermani, S. Kitipornachi, L. Heung-Fai, Modeling and analysis of lattice towers with more accurate models, Advanced Steel Construction 3 (2) (2007) 565–582.
[3] N. Prasad Rao, K. G. M. Samuel, N. Lakshmanan, R. I. Nagesh, Effect of bolt slip on tower deformation, Practice Periodical on Structural Design and Construction 17 (2) (2012) 65–73.
[4] S. Kitipornchai, F. Albermani, A. H. Peyrot, Effect of bolt slippage on ultimate behaviour of lattice structures, Journal of structural engineering 120 (8) (1994) 2281–2287.
[5] W. Jiang, Z. Q. Wang, G. McClure, G. Wang, J. Geng, Accurate modeling of joint effects in lattice transmission towers, Journal of Engineering Structures 33 (2011) 1817–1827.
[6] W.Q. Jiang, Y.P. Liu, Chan SL, Z.Q. Wang, Direct analysis of an ultrahigh-voltage lattice transmission tower considering joint effects. Journal of Structural Engineering (2017) 143(5): 04017009. https://doi.org/10.1061/(ASCE)ST.1943-541X.0001736.
[7] W. Kang, F. Albermani, S. Kitipornchai, H.F. Lam, Modeling and analysis of lattice towers with more accurate models, Advanced Steel Construction. 3 (2007) 565–582.
[8] G. M. S. Knight, A. R. Santhakumar, Joint effects on behaviour of transmission towers, Journal of structural engineering 119 (3) (1993) 698–712.
[9] L. An, J. Wu, W. Jiang, Experimental and numerical study of the axial stiffness of bolted joints in steel lattice transmission tower legs. Engineering Structures (2019) 187: 490-503. https://doi.org/10.1016/j.engstruct.2019.02.070
[10] N. Ungkurapinan, S. S. Chandrakeerthy, R. Rajapakse, S. Yue, Joint slip in steel electric transmission towers, Journal of Engineering Structures 25 (2003) 779–788.
[11] A.H. Abdelrahman, Y.P. Liu, S.L. Chan, Advanced joint slip model for single-angle bolted connections considering various effects. Advances in Structural Engineering (2020) 23(10): 2121-2135. https://doi.org/10.1177/1369433220906226.
[12] H. Gan, H.Z. Deng, C. Li, Simplified joint-slippage model of bolted joint in lattice transmission tower. Structures (2021) 32: 1192-1206. https://doi.org/10.1016/j.istruc.2021.03.022
[13] Q. Cai, R. G. Driver, End tear-out failures of bolted tension members, Tech. Rep. Structural Engineering Report 278, University of Alberta (2008).
[14] Code_Aster Open Source - general FEA software, www.code-aster.org
[15] C. O. Rex, W. S. Easterling, Behavior and modeling of a single plate bearing on a single bolt, Tech. Rep. Rep. CE/VPI-ST 96/14, Virginia Polytechnic Institute and State Univ., Blacksburg, Va. (1996).
[16] G. L. Kulak, et al., Guide to Design Criteria for Bolted and Riveted Joints, AISC, 2001.
[17] SAE Fastener Standards Manual, SAE International - ISBN: 978-0-7680-2170-7, 2009.
[18] C. O. Rex, W. S. Easterling, Behavior and modeling of a bolt bearing on a single plate, Journal of Structural Engineering 129 (6) (2003) 792–800.
[19] ASTM A370-02, Standard Test Methods and Definitions for Mechanical Testing of Steel Products, ASTM International, West Conshohocken, PA, 2001